Fermi National Accelerator Laboratory

Summer Internship Program

High granularity calorimeter studies for a very large hadron collider at 100 TeV: tau lepton tagging at truth level

Donato Farina

Supervisor: Prof. Ashutosh V. Kotwal
Co-supervisors: Dr. Matteo Cremonesi, Dr. Sourav Sen

Final Report - Batavia - September 24 2015

Contents

Abstract

Tau lepton tagging will be a difficult challenge in the very large hadron collider which could be built in the future. Outgoing particles will be very boosted and it will be necessary to have a high granularity calorimeter in order to distinguish different hadronic jets.

Before studying detector response simulations to tau hadronic jets, we have concentrated in the tau tagging at truth level (i.e. knowing particle identities).

In particular we have studied simulations of an electron-positron collision at $500 GeV$, selecting the $e^+ e^- \rightarrow Z^* \rightarrow \tau \tau$ channel.

We have implemented an efficient clustering algorithm for building the two tau-jets stemming from the two tau leptons, which consists in clustering around the particle having the highest transverse momentum.

Also a π^0 reconstruction from the photon pairs has been performed and we have calculated several tau discriminating variables, useful in the discrimination against quark-like jet background.

This work represents a starting point for a more complex study of the tau tagging using detector simulations.

1 Introduction: HL-LHC and FCC

Next projects in hadron collider physics are the high luminosity LHC program (HL-LHC) and the construction of the very large hadron collider at 100 TeV (VLHC).

After 2020, due the radiation effects some critical components of the LHC accelerator will reach their radiation damage limit and also the statistical gain running the collider at constant luminosity will decrease.

For these motivations to study higher energy phenomena, LHC needs to increase its luminosity: this is the goal of the HL-LHC program. In the high luminosity phase, LHC will reach the astonishing threshold of 3000 fb^{-1} of integrated luminosity during its first decade of operation.

It's known that in high energy physics, center of mass energy of the collision and luminosity play a complementary role. In fact the other major program is the realization of the future hadron collider at 100TeV.

We can make some evaluations of the physical quantities which will characterize the future collider.

A large collider radius would lead to two important advantages: less losses by synchrotron radiation in the storage ring and a lower magnetic field.

In fact since the proton momentum is proportional to the collider radius and to the magnetic field, if we take a tunnel lenght R=100km (LHC tunnel is 27 km, see figure 1) we should have a magnetic field about 15T (two times the magnetic field of LHC) for keeping protons in orbit.

It is a difficult challenge to build magnets which work at 15T in operating conditions. Currently in the LHC accelerator niobium titanium superconductor magnets (NbTi), which have a critical temperature of 10K and a

3

critical magnetic field of 15T, are used .

For the collider at 100 TeV, collider physicists probably will use a new superconductor technology which is developing in these years. New triniobium-tin (Nb_3Sn) superconductor technology has an higher critical field than NbTi and also an higher critical temperature (18.3K). These features make this superconductor the major candidate for the construction of the future collider.

In particular an higher critical temperature makes magnets resistant to radiation emissions in the storage ring and an higher magnetic field is important to withstand to the magnetic field of FCC in operating conditions.

Main problem to solve is as usual the power dissipated by synchrotron radiation which will be 20 times LHC. It must be removed at cryogenic temperatures and it is the biggest challenge from a technological point of view.

An important question is surely: why could be important achieve 100TeV or, in general, increase the center of mass energy in particle physics?

Increase center of mass energy means analyze the physics of very massive particles, like the recently discovered Higgs boson, since cross sections of this kind of events generally increase with the energy.

It is interesting to understand for instance up to which level of precision, the Higgs boson behaves like predicted by the standard model. In fact the standard model, being a renormalizable theory, makes very precise predictions about the parameters of the Higgs boson: this makes the measurement of its properties a crucial test to verify the validity of this theory and any discrepancy between theoretical and experimental observations will be an important hint of the existence of new physics.

An other challenge is find the new particles which can explain the phenomena beyond the standard model like neutrino oscillations, dark matter, matter-antimatter asymmetry.

Hence we can say that high energy hadron colliders have been instrumental to discoveries in particle physics at the energy frontier and their role as discovery machines will remain unchallenged for the foreseeable future [1].

2 Tau lepton tagging

2.1 Tau lepton in high energy physics

This work concerns tau lepton tagging. Tau lepton is an important particle in high energy physics: it is the heaviest lepton, with an invariant mass of 1.777 GeV, and so it is involved in a lot of processes at very high energies. For example it was predicted and recently experimentally verified that Higgs boson can decay into two tau leptons
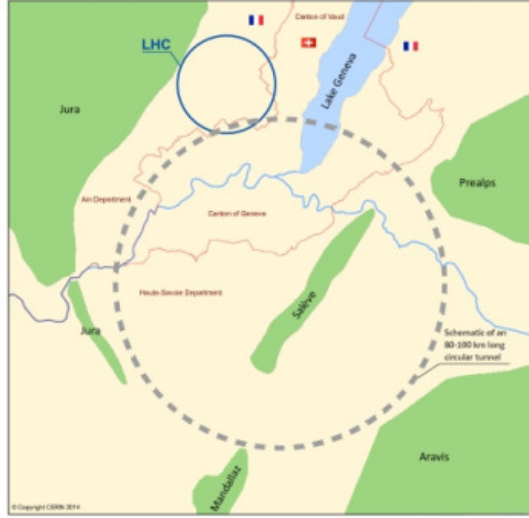
$$H \to \tau^+ \tau^-,$$

Figure 1: Map of the Very Large Hadron Collider (VLHC) and its location compared to the Large Hadron Collider (LHC).

hence tau tagging is important for a deeper understanding of the Higgs physics.

Other typical processes which involve tau lepton are the decays of W and Z bosons, the elementary particles which mediate the weak interaction

$$W \to \tau \, \nu_\tau$$

$$Z \to \tau^+ \, \tau^-.$$

An other important characteristic is that tau life time is very short, about $10^{-13}s$, so actually in the ATLAS detector at LHC is not detected tau lepton, but its decay products. Due its great mass tau lepton can decay either leptonically or hadronically:

$$\tau \to l \, \nu_\tau \, \nu_l$$

$$\tau \to hadrons \, \nu_\tau.$$

We are interested in the hadronic channel, since in order to distinguish a tau lepton hadronic jet from a quark-like jet will be a difficult challenge in the future collider: an high granularity calorimeter will be necessary in the future collider. In fact, increasing the center of mass energy, particles will be more boosted and so their jets more superimposed so that a very high spatial resolution will be needed.

2.2 Tau reconstruction in ATLAS

A great effort in the ATLAS group is concentrated in the tau lepton reconstruction studies, where *reconstruction* means an identification, working with a signal below the trigger threshold.

Sources of noise are as usual electronic noise and the pile-up effects (superposition of signals very close temporally), but it is generally simple to suppress them using the Topocluster algorithm: Topocluster algorithm builds the jets, clustering in an iterative way around a seed track, following some energy significance criteria, and can split superimposed jets.

The problem is that it doesn't suppress the quark-like jet noise since these jets have characteristics very similar to the tau lepton ones: they are very collimated and have few tracks.

For this aim Topocluster algorithm works only as input of a more complex identification process. It is followed by the anti-K_t algoritm which leads to choose *tau hadron visible candidates* between all jets which are present in the collision event.

This algorithm applies some selection criteria for finding these candidates, based on the number of associated tracks, which in a tau hadronic decay is one or three, transverse momentum of the jet $P_t > 10 GeV$ (or some other threshold of this order of magnitude) and its pseudorapidity $\eta < 2.5$.

Also, it leads to the tau hadron primary vertex which is used in order to find the jet direction. In the primary vertex is built the coordinate system where the identification variables will be defined.

Finally for the discrimination against quark-like jets other variables are used. They are like signatures of the two different events and for this motivation they are called discriminating variables.

For example the *central energy fraction*, defined as the ratio between the transverse energy deposited in the region $\Delta R < 0.1$ and the energy deposited in the region $\Delta R < 0.2$ around the jet direction, is a quantity which has generally a different histogram if we consider a tau hadronic jet or a quark-like jet and, for this reason, it is considered a good discriminating variable, suitable in order to reject the quark-like jet background.

There are a lot of other discriminating variables, like the *number of tracks in the isolation region* or the *maximum ΔR in the core region*. For a more complete list one can look ref. [2].

3 Analysis of simulated $Z \to \tau^+ \tau^-$ events at truth level

3.1 Monte Carlo event simulation

Use of hadron colliders has advantages and disadvantages. Since the energy losses by synchrotron radiation are proportional to m^{-3} they allow to reach higher energies than the electron-positron colliders, in which emission radiation is much more intensive. The problem is that protons are not elementary particles, since they are composed by quarks which interact by mean the strong force. Using hadron colliders we don't know exactly which elementary particles have actually interacted during the collision and their initial energies. This implies some difficulties in the data analysis.

Electron-positron collider studies, since electron and positron are elementary particle, are more suitable for understanding quickly many physical concepts. Currently we are concentrating in the tau lepton tagging at truth level, i.e. knowing the identities of the final state particles, before studying detector response using simulations.

We have as input Monte Carlo event simulation of an electron-positron collision at 500 GeV center of mass energy.

In particular we have made a cut on the events selecting only the decay channel

$$e^+ e^- \to Z^* \to \tau^+ \tau^-.$$

We have 10000 events of this kind and we have access to the four momenta and the particle identity numbers (PIDs) of the outgoing stable particles of each event stemming from the two tau decays.

The particles which we can find in our data are written in table 1 together with their PIDs. From the PIDs we have deduced the charge of the particles, which is also listed in the table.

Looking at particle identity numbers we can see that we have in the file events.dat all the tau lepton decay products except neutral pions.

In fact events.dat contains only stable particles: a neutral pion, having a very short life time, cannot be detected and it has to be reconstructed from its decay products, mostly photon pairs

$$\pi^0 \to \gamma \gamma.$$

The first work has been to build the two jets, which we call $jet^{(A)}$ and $jet^{(B)}$, stemming from the two tau leptons respectively.

We define the angular distance (or simply distance) between two particles, say 1 and 2, in the following way:

$$\Delta R_{1\,2} = \sqrt{(\eta_1 - \eta_2)^2 + (\phi_1 - \phi_2)^2},$$

PID	particle	charge
-16	$\bar{\nu}_\tau$	0
-14	$\bar{\nu}_\mu$	0
-13	μ^+	1
-12	$\bar{\nu}_e$	0
-11	e^+	1
11	e^-	-1
12	ν_e	0
13	μ^-	-1
14	ν_μ	0
16	ν_τ	0
22	γ	0
130	K^0_L	0
211	π^+	1
-211	π^-	-1
310	K^0_S	0
321	K^+	1
-321	K^-	-1

Table 1: Particle identity numbers (PIDs) and charges of the particles present in events.dat.

where ϕ_i is the azimutal angle of the i particle around the beam direction (z axis) and η_i is the pseudorapidity of the i particle, defined as

$$\eta = -\ln(\tan(\theta/2)).$$

In order to verify that we really have two jets, estimate the typical angular distance between the two jets and their typical width, we have plotted the distances which characterize all pairs of particles, ΔR_{ij}. The corresponding histogram is shown in figure 2.

We can deduce from figure 2 that almost all jet's particles are in the cone $\Delta R < 0.6$ around the jet axis, which we define as the direction of the jet three-momentum.

3.2 Splitting into two jets

We want to describe briefly the algorithm which we have implemented, it consists in a simple and efficient procedure which splits event particles into two jets.

We find at first a particle seed around which we start the clustering procedure. The particle seed can be the particle having the highest energy (E_{max} clustering) or the highest transverse momentum ($P_{t\,max}$ clustering), or it can be a tau-neutrino since every jet has to contain one and only one tau neutrino.

The last choice is not close to the common experimental procedure, since neutrinos are not detected in the ATLAS detector and they are observed indirectly as missing transverse energy. However at truth level it is a reasonable choice and it helps us to understand which clustering method is more appropriate between the E_{max} and $P_{t\,max}$ algorithms.

After we have found the seed particle, we take it as the jet direction and we add to the jet all particles in the cone $\Delta R < 0.6$ around the jet direction.

Once built the $jet^{(A)}$ we redefine the jet direction as the direction of the jet tri-momentum and we repeat the same procedure for building the $jet^{(B)}$: between the remaining particles we find the particle seed and we add to the $jet^{(B)}$ the particles which have a tri-momentum in the cone $\Delta R < 0.6$ around the seed axis and at the end we define the $jet^{(B)}$ direction as the direction of the $jet^{(B)}$ tri-momentum.

Looking the plots of the sum of the energies of the two jets and the transverse component of the total tri-momentum of the two jets we can understand what are the advantages and the disadvantages of the two clustering algorithms, namely E_{max} and $P_{t\,max}$ algorithms.

Using the $P_{t\,max}$ algorithm, selecting surely the two particles with the highest transverse momentum, the momentum balance is well achieved and we can see only a peak at 0 GeV in figure 3. But if we look at the total energy in figure 4 we can see two peaks: one expected at 500 GeV and another peak at about 260 GeV. This means that some highly energetic particles are not included in the two jets using the $P_{t\,max}$ algorithm.

On the other hand if we use the E_{max} algorithm we can see that the energy balance is well guaranteed but the momentum balance is not so good compared to the $P_{t\,max}$ one (figures 5 and 6, respectively).

The clustering around neutrinos is the key to choose what is the more appropriate method in this case. We have calculated at first the distance between the two tau neutrinos, which we plot in figure 7.

We can see in figure 7 that we obtain a peak around 3.6, about the same result obtained when we plotted the distances between every pair of particles in every event (figure 2), where 3.6 was the distance between the two peaks. It is a confirmation that to plot the distances that characterize every pair of particles has been a good idea for estimating the distance between the two jets and their width.

In fact the angular distance between the two tau neutrinos $\Delta R = 3.6$ represents an estimation of the mean distance of the two jets since the two jets are characterized always by a tau-neutrino and an anti-tauneutrino respectively. After we have clustered around the two neutrinos, we can study again the distributions of the total energy of the two jets and the transverse component of the total momentum of the two jets.

We have obtained very similar results to the $P_{t\,max}$ ones: for example in the E_{tot} graph (see figure 8) we can observe again the peak at 260 GeV, already observed using the $P_{t\,max}$ algorithm. Also, an other confirmation that the
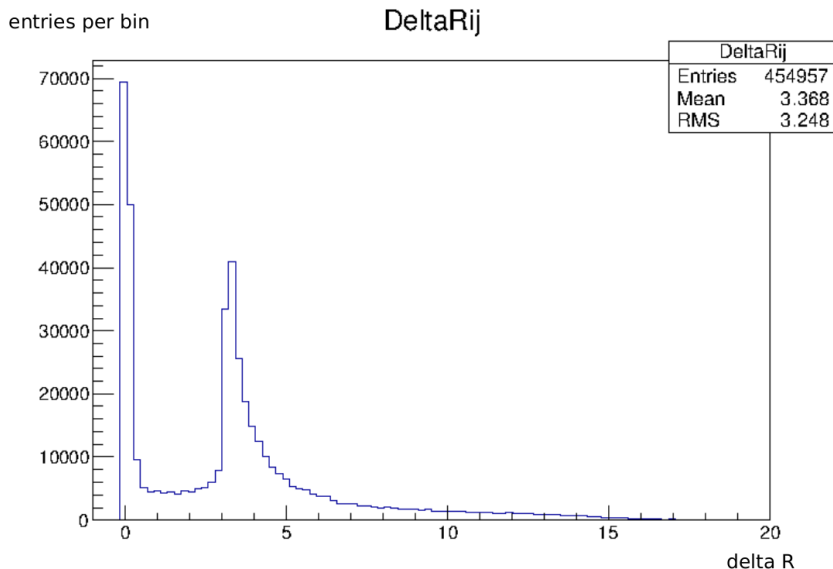
9

Figure 2: Angular distance between every pair of particles present in each event.

P_{tmax} algorithm is more efficient than the E_{max} one is that the mass of the jet in the first case is consistent with the tau-lepton mass, conversely in the second case it is not consistent and we can observe also an unexpected peak around 0.2 GeV (see figures 9 and 10).

A reasonable explanation is that in the event file we have some highly energetic photons stemming from the incoming electrons by synchrotron radiation, hence they don't belong to the two outgoing tau-jets and it would be wrong to cluster around them.

Also, we have analized the pseudorapidity distributions of the jets and the invariant mass of the system composed from the two tau jets (dijet system) using the two clustering methods.

In figures 11 and 12 we can see that the E_{max} algorithm looks like include erroneously initial state radiation photons more frequently than the P_{tmax} one, since its distribution has an higher width (initial state radiation photons generally have momenta very close to the beam axis, hence high pseudorapidity).

In figure 14 we obtain again a more reasonable result about the dijet mass: the P_{tmax} algorithm yields two peaks one at the Z boson mass, real Z boson, and the other at 500 GeV, virtual Z boson.

In conclusion for the calculation of the tau discriminating variables we have chosen the P_{tmax} algorithm since it works better than the E_{max} algorithm at truth level (even though at experimental level the clustering is usually made using energy significance criteria, see ref. [3]).
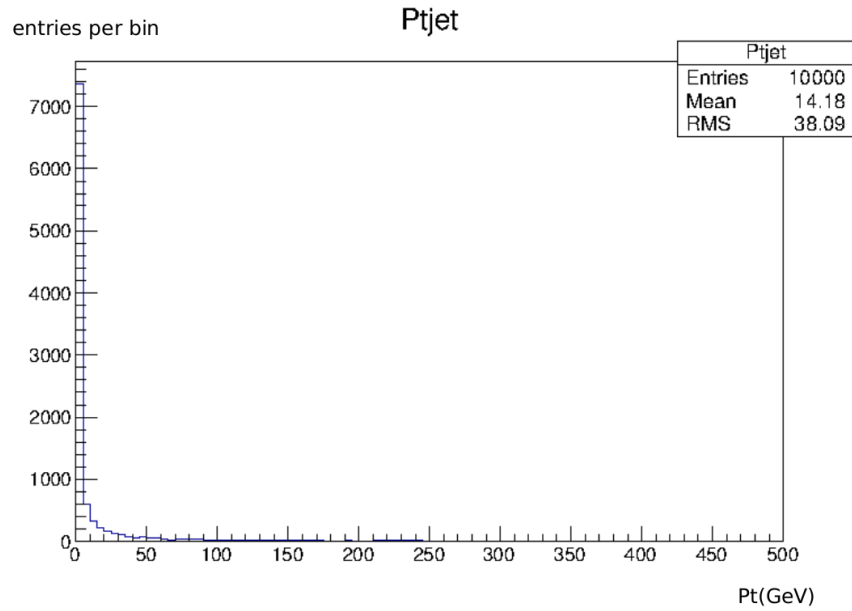
Figure 3: Transverse component of the total trimomentum of the two jets, clustering around the $P_{t\,max}$ particle.
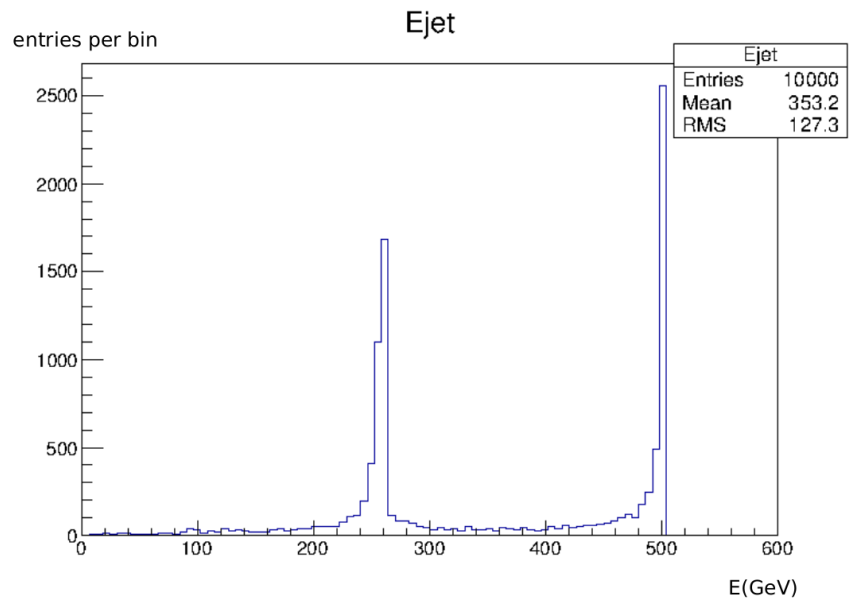

Figure 4: Sum of the energies of the two jets, clustering around the $P_{t\,max}$ particle.
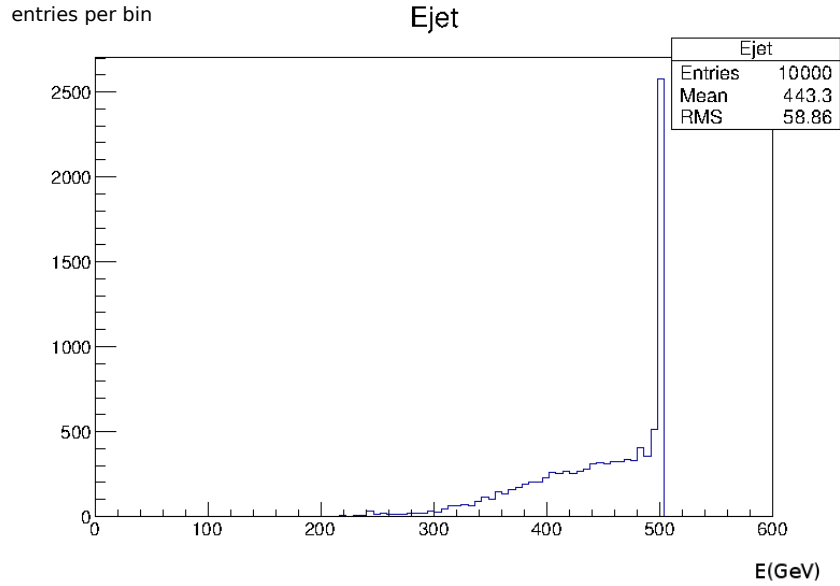
11

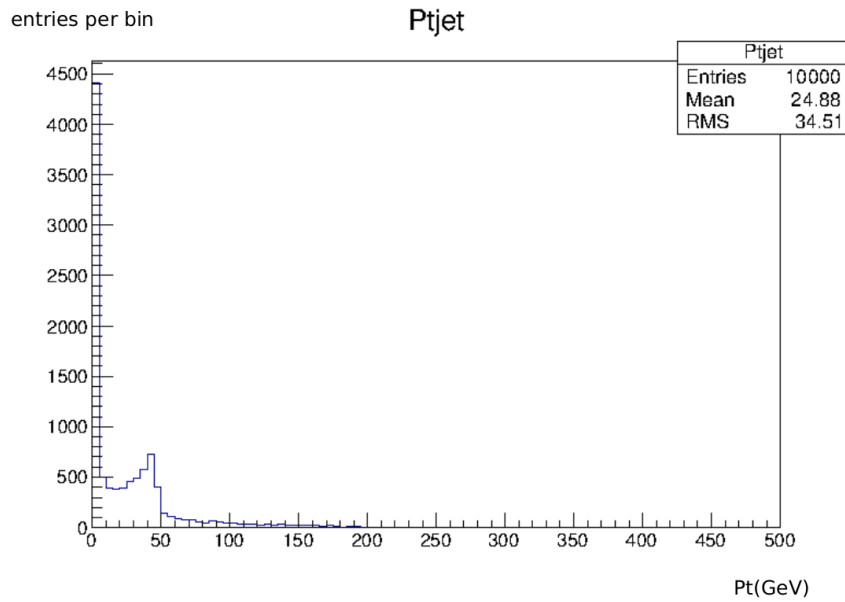Figure 5: Sum of the energies of the two jets, clustering around the E_{max} particle.

Figure 6: Transverse component of the total trimomentum of the two jets, clustering around the E_{max} particle.
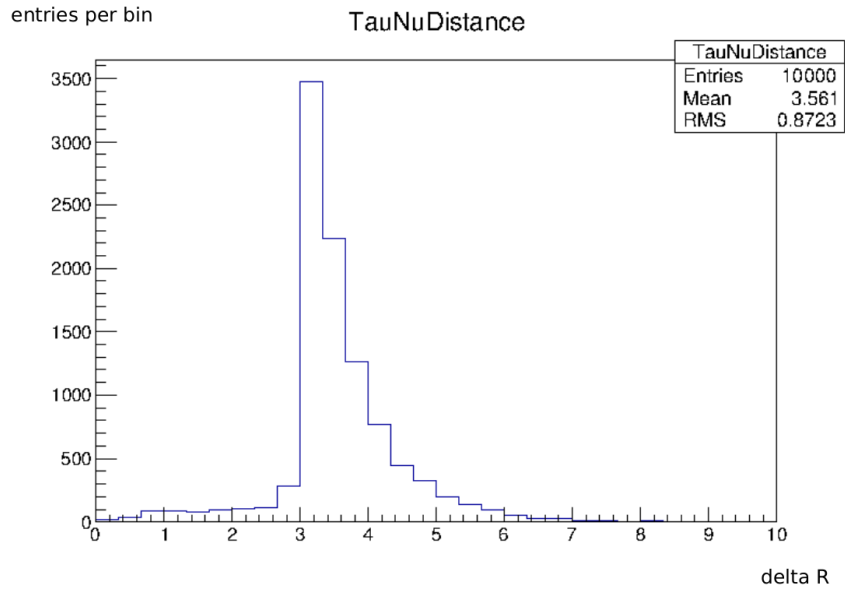
12

Figure 7: Distance between the two tau neutrinos.
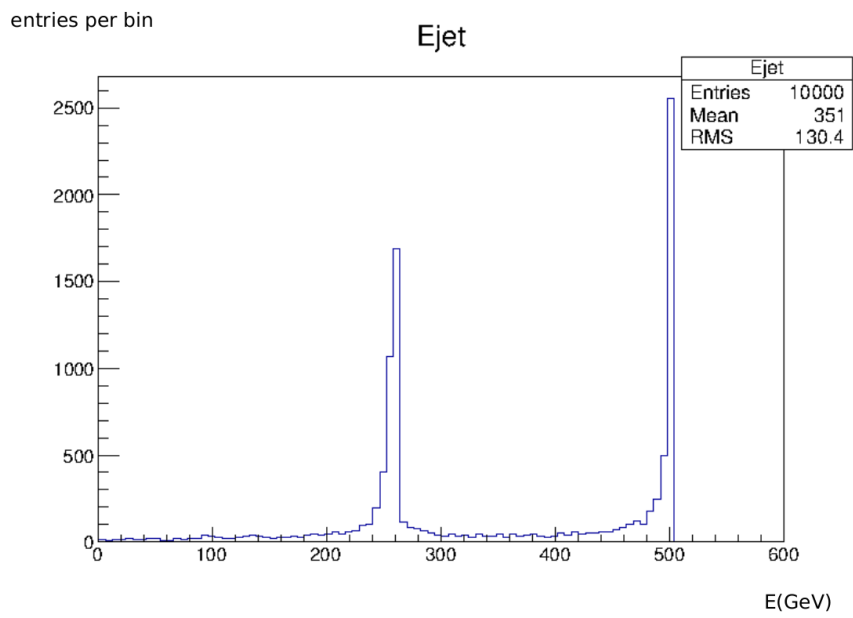
Figure 8: Sum of the energies of the two jets, clustering around the two tau neutrinos.

13
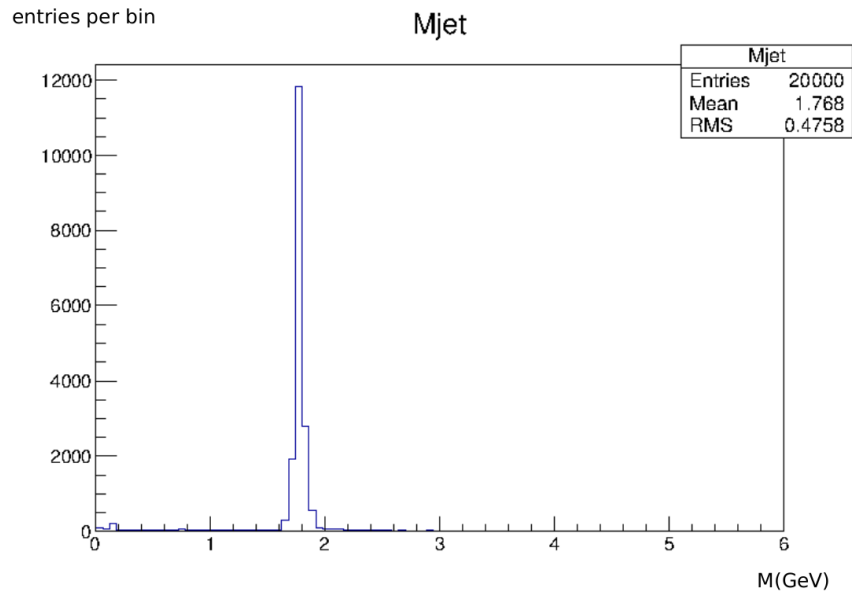
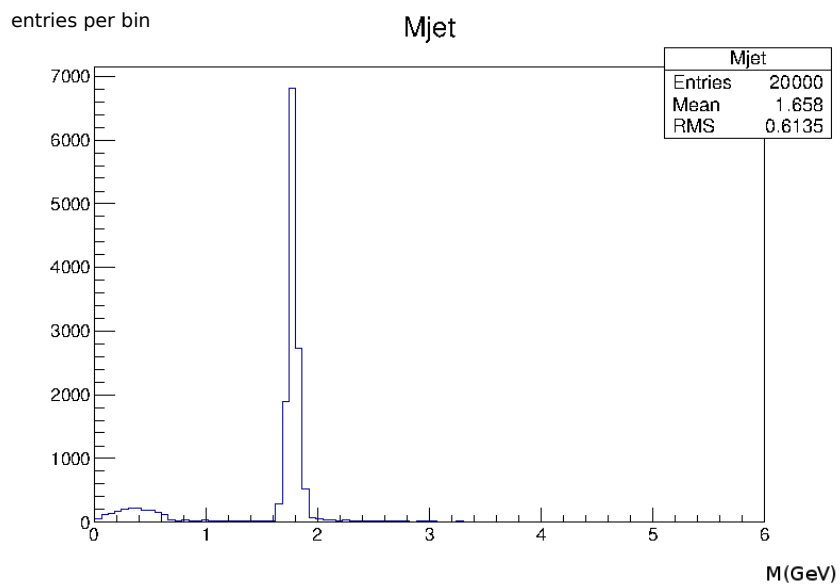Figure 9: Invariant mass of the jet, clustering around the $P_{t\,max}$ particle.

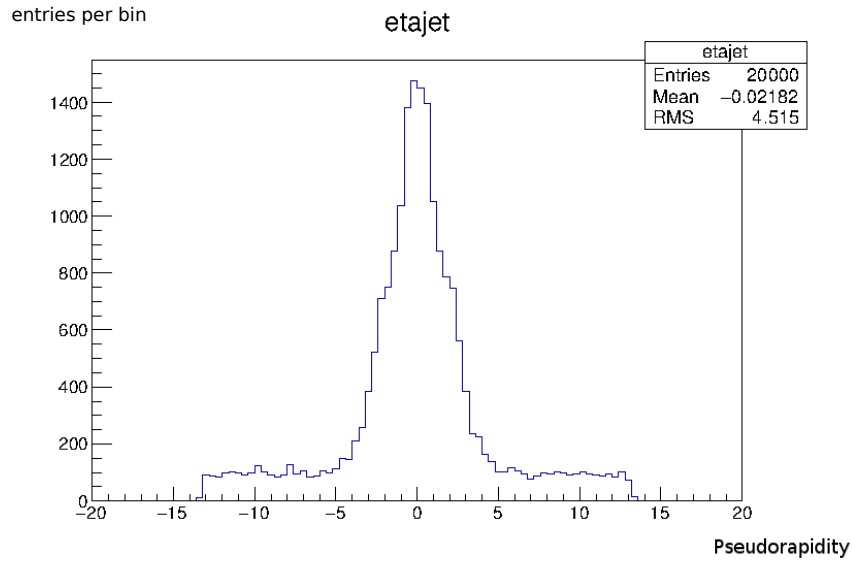Figure 10: Invariant mass of the jet, clustering around the E_{max} particle.

Figure 11: Distribution of the jet pseudorapidity, obtained by using the E_{max} clustering method.
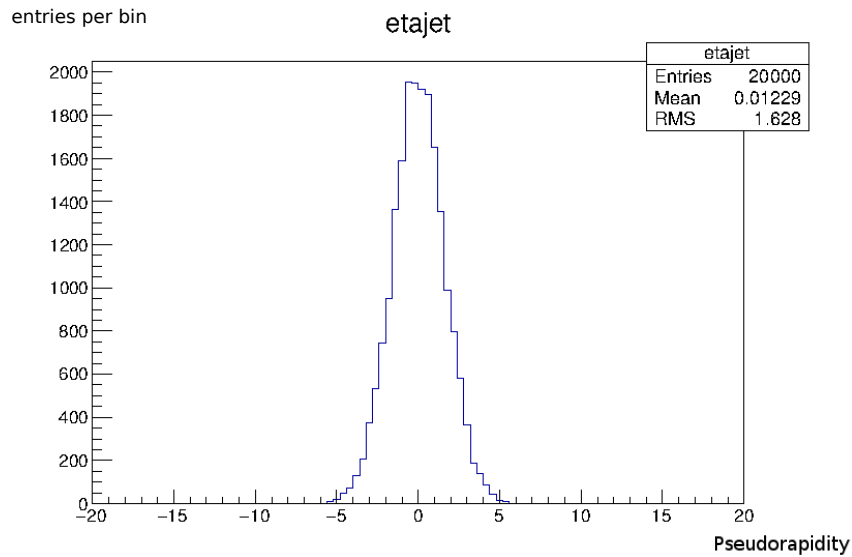

Figure 12: Distribution of the jet pseudorapidity, obtained by using the $P_{t\,max}$ clustering method.
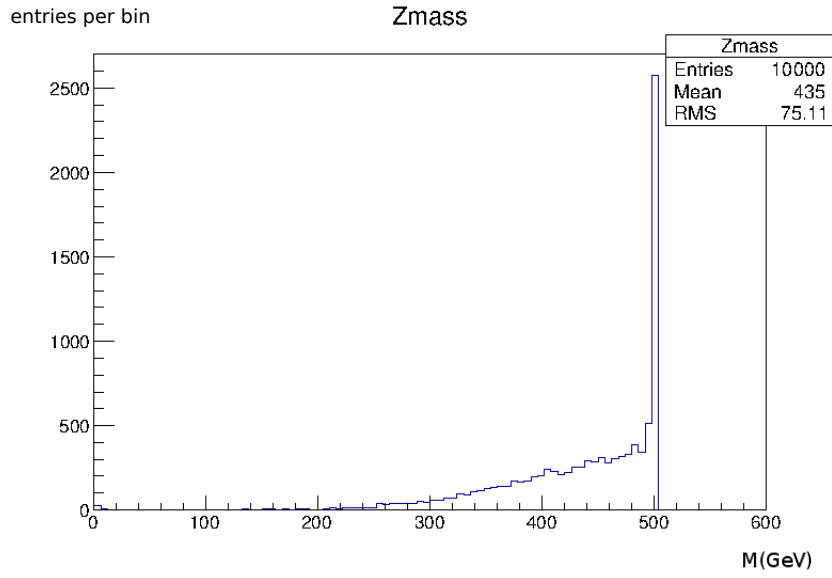
15

Figure 13: Invariant mass of the dijet system, obtained by using the E_{max} clustering method.
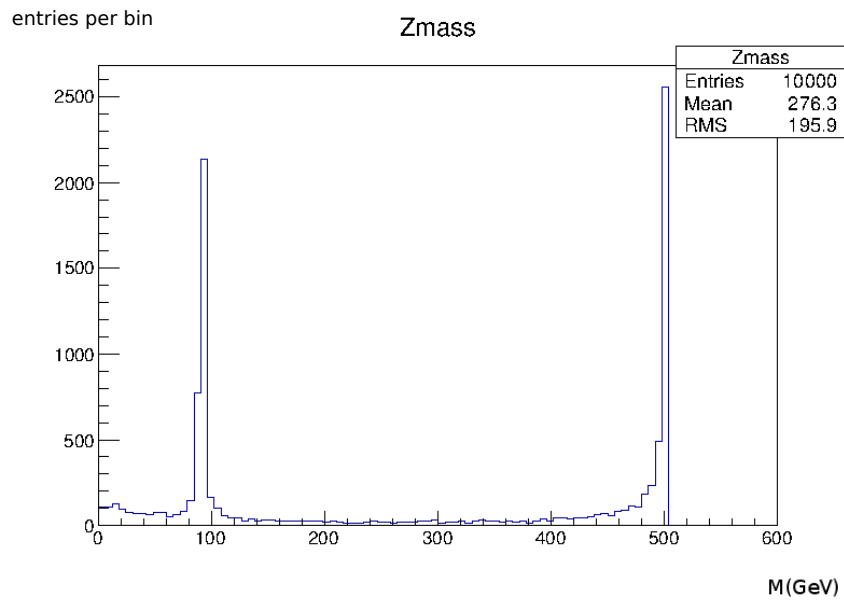

Figure 14: Invariant mass of the dijet system, obtained by using the $P_{t\,max}$ clustering method.

16

3.3 Tau reconstruction: discriminating variables

Once we have built the two tau jets using the $P_{t\,max}$ algorithm, we have rejected all jets which contain an electron or a muon or their corresponding neutrinos, since we are interested in the hadronic channel.

At this point the work is consisted in calculating the tau-lepton discriminating variables, which are like a signature of this particle, very useful for the discrimination against quark-like jets.

We list below the definitions of such discriminating variables and the corresponding distributions which we have obtained.

Also, a π^0 reconstruction has been performed coupling photon pairs in a reasonable way. The corresponding algorithm will be explained when we will treat the *number of reconstructed π^0 in the core region*, one of these discriminating variables.

- **Central energy fraction** (figure 15): ratio of the transverse energy deposited in the region $\Delta R < 0.1$ and the energy deposited in $\Delta R < 0.2$ around the jet direction, taking only jets with a pseudorapidity $\eta < 2.5$, $P_t > 15 GeV$, with one associated track (i.e. one charged particle in the hadronic decay).

- **Number of tracks in the isolation region** (figure 16): number of charged particles in the isolation region around the jet direction, which is defined as the region $0.2 < \Delta R < 0.4$, taking only jets with a pseudorapidity $\eta < 2.5$, $P_t > 15 GeV$, with one associated track.
  Since we have selected the only one track hadronic decays we have just two peaks at 0 and at 1. We can see that the majority of the tracks are not in the isolation region, being very close to the jet direction.

- **Maximum ΔR in the core region** (figure 17): maximum ΔR considering only the tracks in the core region ($\Delta R < 0.2$), taking only jets with a pseudorapidity $\eta < 2.5$, $P_t > 15 GeV$, with three associated tracks.
  This histogram shows that the tracks are very close to the jet axis, with a peak at 0.02, consistently with the graph 16.

- **Number of reconstructed π^0 in the core region** (figure 18): number of reconstructed π^0 in the core region, considering only the jets with a pseudorapidity $\eta < 2.5$, $P_t > 15 GeV$, with one associated track.
  The algorithm, which we have implemented to obtain a π^0 reconstruction, works in the following way.
  In the region $\Delta R < 0.6$ around the jet axis, it finds the photon pair which has the closest total momentum to the jet axis. If a such pair exists, we increase by one the number of reconstructed π^0 and, considering the remaining photons, we repeat the same procedure in order to find an other π^0 pair. We repeat this procedure iteratively up to
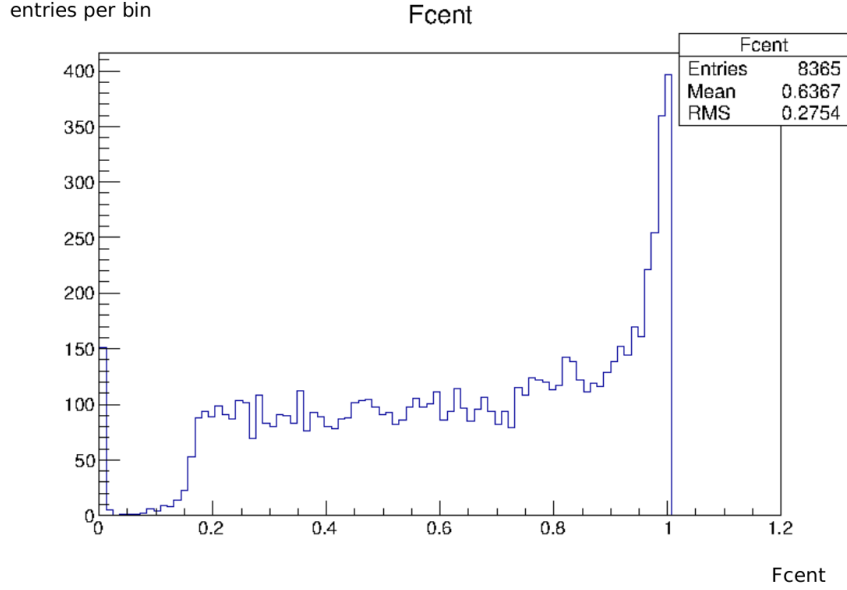
Figure 15: Central energy fraction.

complete the π^0 reconstruction.

We have obtained a qualitative good result, since the histogram reproduces the correct hierarchy between the four peaks: the highest peak is at 1 and the lowest is at 3, the peaks at 2 and 0 have similar hight as expected from the theory.

- **R_{track}** (figure 19): p_t-weighted mean distance between the tracks, in the core and isolation, region and the tau jet direction, considering only the jets with a pseudorapidity $\eta < 2.5$, $P_t > 15 GeV$, with 3 associated tracks.

- **M_{track}** (figure 20): invariant mass of the tracks in the core and isolation regions, assuming a pion mass for each track, considering only the jets with a pseudorapidity<2.5, P_t>15 GeV, with 3 associated tracks.

- **F_{track}** (figure 21): the highest p_t between the tracks in the core region divided by the transverse energy sum in the core region, considering only the jets with a pseudorapidity $\eta < 2.5$, $P_t > 15 GeV$, with 3 associated tracks.
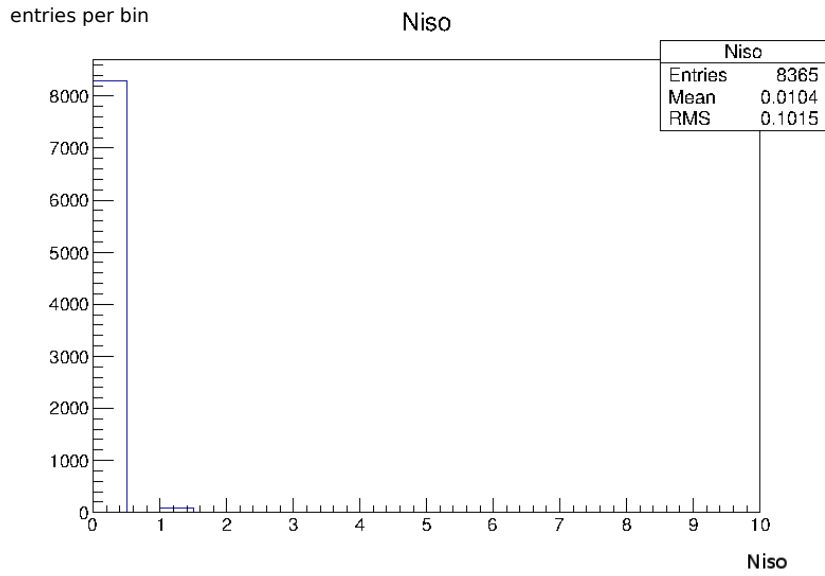
entries per bin

Niso

Niso	
Entries	8365
Mean	0.0104
RMS	0.1015

Niso

Figure 16: Number of tracks in the isolation region.

entries per bin

MaxDeltaR

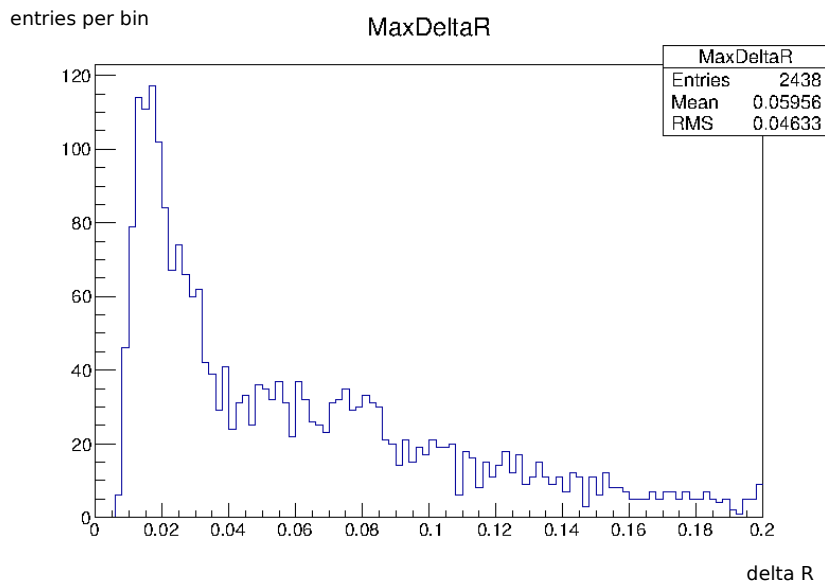| MaxDeltaR	
Entries	2438
Mean	0.05956
RMS	0.04633

delta R

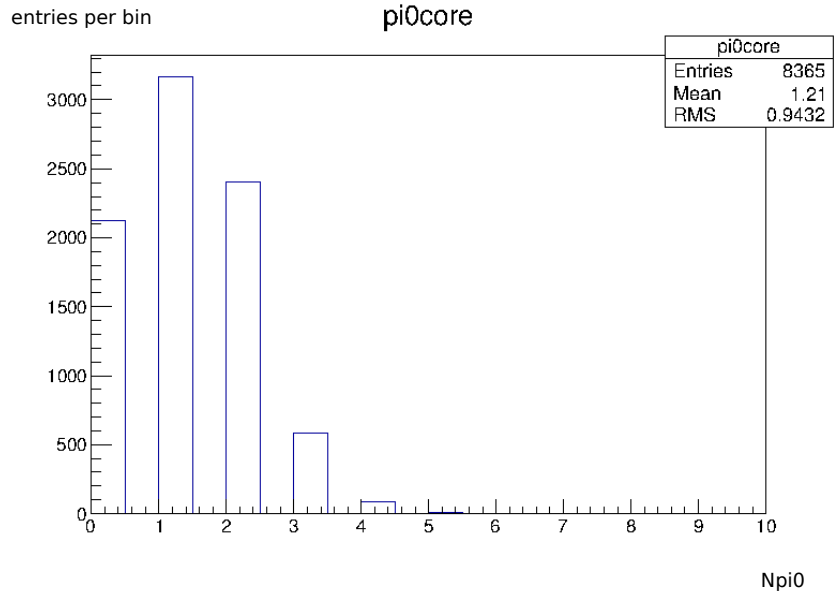Figure 17: Maximum ΔR in the core region.
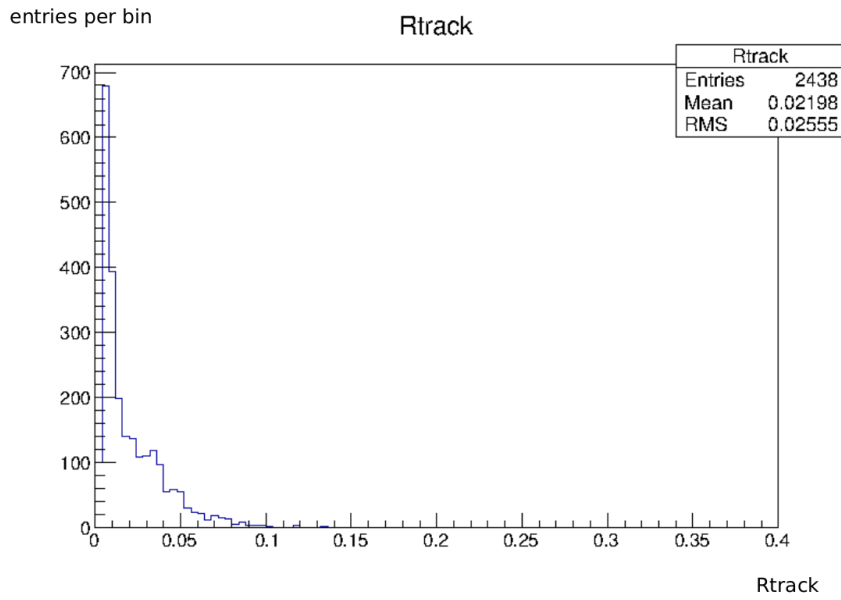
Figure 18: Number of reconstructed π^0 in the core region.

Figure 19: p_t-weighted mean distance between the tracks, in the core and isolation, and the tau jet direction .
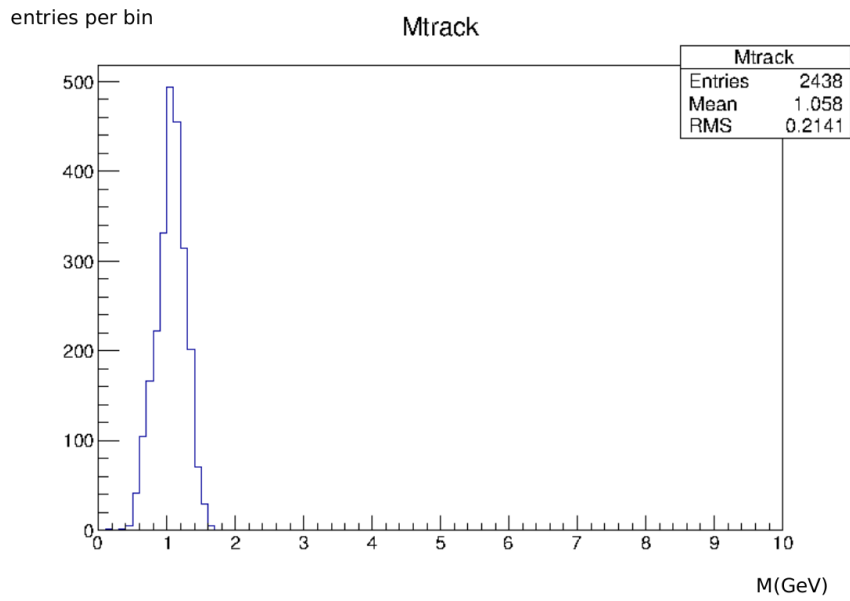
entries per bin

Mtrack

Mtrack	
Entries	2438
Mean	1.058
RMS	0.2141

M(GeV)

Figure 20: Invariant mass of the tracks in the core and isolation regions, assuming a pion mass for each track.

entries per bin

Ftrack

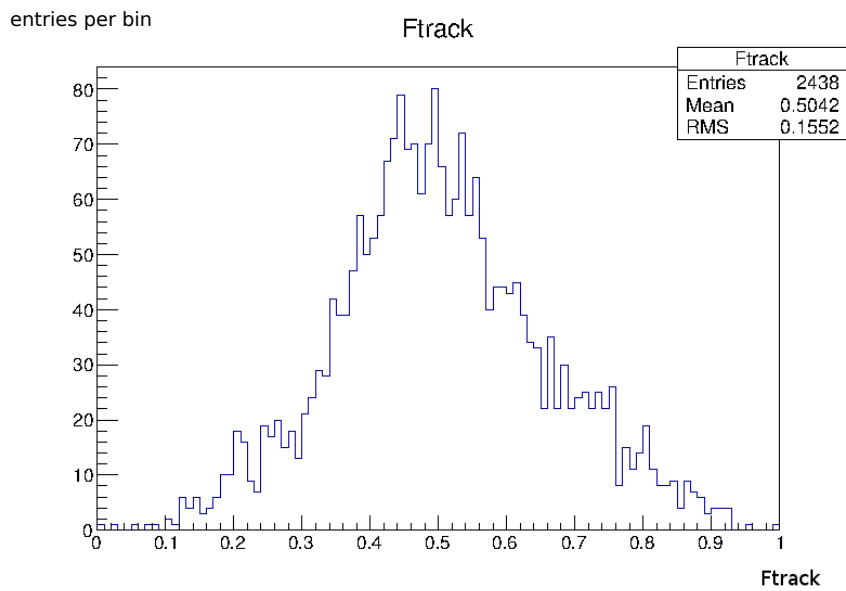| Ftrack	
Entries	2438
Mean	0.5042
RMS	0.1552

Ftrack

Figure 21: The highest p_t between the tracks in the core region divided by the transverse energy sum in the core region.

4   Summary and results

Tau lepton tagging will be a difficult challenge in the very large hadron collider which could be built in the future. Outgoing particles will be very boosted and it will be necessary to have a high granularity calorimeter in order to distinguish different hadronic jets.

Before studying detector response simulations to tau hadronic jets, we have concentrated in the tau tagging at truth level (i.e. knowing particle identities).

In particular we have studied simulations of an electron-positron collision at $500GeV$, selecting the $e^+ e^- \rightarrow Z^* \rightarrow \tau^+ \tau^-$ channel.

We have implemented an efficient clustering algorithm for building the two tau-jets stemming from the two tau leptons, which consists in clustering around the particle having the highest transverse momentum.

Also a π^0 reconstruction from the photon pairs has been performed and we have calculated several discriminating variables, useful for the discrimination against quark-like jets: central energy fraction; number of tracks in the isolation region; maximum ΔR in the core region; number of reconstructed π^0 in the core region; p_t-weighted mean distance between the tracks, in the core and isolation, and the jet's direction; invariant mass of the tracks in the core and isolation regions, assuming a pion mass for each track; the highest p_t between the tracks in the core region divided by the transverse energy sum in the core region.

This work represents a starting point for a more complex study of the tau tagging using detector simulations.

5   References

[1]Barletta, William, et al. "Future hadron colliders: From physics perspectives to technology R e D." Nuclear Instruments and Methods in Physics Research Section A: Accelerators, Spectrometers, Detectors and Associated Equipment 764 (2014): $352 - 368$.

[2]ATLAS collaboration. "Identification and energy calibration of hadronically decaying tau leptons with the ATLAS experiment in pp collisions at $\sqrt{s}=$ 8 TeV." arXiv preprint arXiv:1412.7086 (2014).

[3]Lampl, W., et al. Calorimeter Clustering Algorithms. No. ATL-LARG-PUB-2008-002. 2008.